

# A Linear Class AB Single-Ended to Differential Transconverter Suitable for RF Circuits

Jeff Durec and Eric Main  
Motorola Inc., 2100 E Elliot Rd., Tempe, AZ 85284

**Abstract-** A novel circuit topology is presented which converts a single-ended signal into differential output currents with improved linearity. This cell operates in Class AB, allowing an output current greater than the quiescent current. A configuration which allows for the nulling of the third order distortion is derived and the implications of third order nulling on third order intermodulation is explained. Measured results of this cell implemented in 0.4  $\mu\text{m}$  silicon-bipolar technology is presented.

## I. INTRODUCTION

Differential transconverter cells are widely used building blocks. Areas which require this type of cell with the added requirement of high linearity and low noise include filters, multipliers and frequency mixers. Typically, high linearity comes at the price of increased current or increased noise. It is of particular interest to design a transconverter which has high linearity, low quiescent current, low noise contribution and large peak available current. In many applications, it is also necessary for the transconverter to have a low input impedance,  $50\Omega$  is a typical requirement for RF circuits.

## II. AMPLIFIER DISTORTION THEORY

The nonlinearities in the transfer function of an amplifier can be expressed as a power series [ 1 ], [ 2 ]:

$$y = f(x) \Rightarrow y = \sum_{n=0}^{\infty} C_n x^n \quad (1)$$

$$y = C_0 + C_1 x + C_2 x^2 + C_3 x^3 + C_4 x^4 + \dots \quad (2)$$

$$C_n = \frac{1}{n!} \left. \left( \frac{d^n}{dx^n} y(x) \right) \right|_{x=0} \quad (3)$$

Harmonic and intermodulation distortion can be calculated from the power series coefficients. If two tones ( 4 ) are applied at the amplifier input then the resulting output will be ( 5 ).

$$x(t) = A_1 \cos(\omega_1 t) + A_2 \cos(\omega_2 t) \quad (4)$$

$$y(t) = DC + F(t) + HD2(t) + IM2(t) + HD3(t) + IM3(t) + \dots \quad (5)$$

Define: DC  $\equiv$  DC output

F(t)  $\equiv$  fundamental components

HD2(t)  $\equiv$  second harmonic distortion product

IM2(t)  $\equiv$  second order intermodulation product

HD3(t)  $\equiv$  third harmonic distortion product

IM3(t)  $\equiv$  third order intermodulation product

These components can be expanded as follows:

$$F(t) = \dots \quad (6)$$

$$\begin{aligned} & \left( C_1 A_1 + \frac{3}{4} C_3 A_1^3 + \frac{3}{2} C_3 A_1 A_2^2 + \frac{5}{8} C_5 A_1^5 + \frac{15}{4} C_5 A_1^3 A_2^2 + \frac{15}{8} C_5 A_1 A_2^4 \right) \cos(\omega_1 t) + \\ & \left( C_1 A_2 + \frac{3}{4} C_3 A_2^3 + \frac{3}{2} C_3 A_1^2 A_2 + \frac{5}{8} C_5 A_2^5 + \frac{15}{4} C_5 A_1^2 A_2^3 + \frac{15}{8} C_5 A_1^4 A_2 \right) \cos(\omega_2 t) + \\ & \dots \end{aligned}$$

$$\begin{aligned} HD2(t) = & \\ \left( \frac{1}{2} C_2 A_1^2 + \frac{1}{2} C_4 A_1^4 + \frac{3}{2} C_4 A_1^2 A_2^2 + \dots \right) & \cos(2\omega_1 t) + \\ \left( \frac{1}{2} C_2 A_2^2 + \frac{1}{2} C_4 A_2^4 + \frac{3}{2} C_4 A_1^2 A_2^2 + \dots \right) & \cos(2\omega_2 t) \end{aligned} \quad (7)$$

$$\begin{aligned} IM2(t) = & \\ \left( C_2 A_1 A_2 + \frac{3}{2} C_4 A_1^3 A_2 + \frac{3}{2} C_4 A_1 A_2^3 + \dots \right) & \cos(\omega_1 t \pm \omega_2 t) + \\ HD3(t) = & \\ \left( \frac{1}{4} C_3 A_1^3 + \frac{5}{16} C_5 A_1^5 + \frac{5}{8} C_5 A_1^3 A_2^2 + \dots \right) & \cos(3\omega_1 t) + \\ \left( \frac{1}{4} C_3 A_2^3 + \frac{5}{16} C_5 A_2^5 + \frac{5}{8} C_5 A_1^2 A_2^3 + \dots \right) & \cos(3\omega_2 t) \end{aligned} \quad (8)$$

$$\begin{aligned} IM3(t) = & \\ \left( \frac{3}{4} C_3 A_1^2 A_2 + \frac{5}{4} C_5 A_1^4 A_2 + \frac{15}{8} C_5 A_1^2 A_2^3 + \dots \right) & \cos(2\omega_1 t \pm \omega_2 t) + \\ \left( \frac{3}{4} C_3 A_1 A_2^2 + \frac{5}{4} C_5 A_1 A_2^4 + \frac{15}{8} C_5 A_1^3 A_2^2 + \dots \right) & \cos(\omega_1 t \pm 2\omega_2 t) \end{aligned} \quad (10)$$

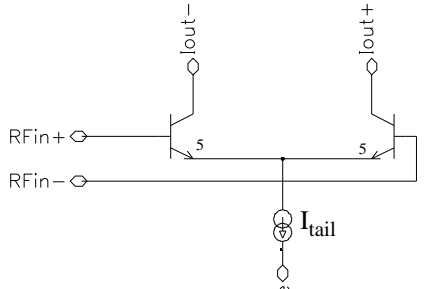
In communication circuits where a single channel needs to be distinguished from adjacent channels, intermodulation can cause great problems. Intermodulation arises when there are two adjacent channels which are much stronger than the wanted signal. After amplification through a nonlinear amplifier, the two adjacent channels can intermodulate and appear on the wanted channel. The wanted signal is then overcome by the intermodulation product.

The third order intermodulation product (IM3) is of particular interest because it is typically the strongest of the odd order intermodulation products. Only the odd order intermodulation components cause the adjacent channel problem. The even order components give outputs which are typically out of the band of interest. A circuit topology which minimizes the third order intermodulation product of an amplifier is greatly desired.

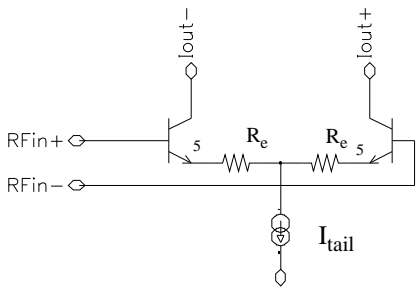
## III. CIRCUIT DESIGN

For high linearity differential transconverter circuits a variation of the differential pair is often used (Fig. 1(A)). Most variants trade linearity for transconductance and noise. The transconductance of this circuit follows the hyperbolic tangent function. A linearization method which uses emitter degeneration is shown in Fig. 1(B). Degeneration resistance is used to absorb some of the input signal. In doing so, the linear range is improved but the transconductance suffers and the noise increases. Fig. 1(C) depicts another method which uses degeneration to improve linearity. This example has the same drawbacks as Fig. 1(B).

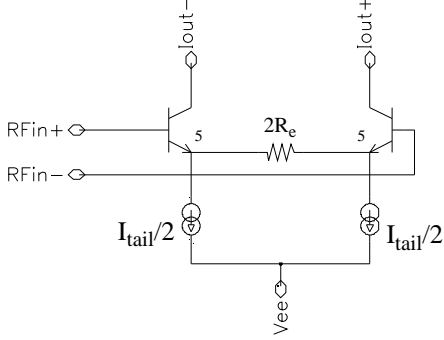
The cell in Fig. 2 utilizes two offset transfer functions that, when summed, yield a higher dynamic range. This improvement arrives at the expense of decreased transconductance and higher noise figure with a net improvement over the differential pair with or without degeneration.



(A) differential pair



(B) degenerated differential pair



(C) degenerated differential pair

Fig. 1. Variations of a differential pair transconductor

Each of the above mentioned variations of the differential pair feature improved linearity but none of them arrive at this without a degradation in noise and a reduction in transconductance. The peak output current is limited to the quiescent current in each of these circuits. In addition, none of these variants feature a method of reducing the input impedance.

Fig. 3 shows an improved transconverter cell<sup>1</sup>. The features of this cell include:

- High linearity
- Low noise
- High peak current
- Low quiescent current
- Good transconductance
- Selectable input impedance
- Single ended drive
- Differential output

This circuit utilizes a common base transistor ( $Q_4$ ) and a current mirror ( $Q_5, Q_6$ ). When current flows through the input, it adds to the quiescent current going through the mirror thus raising the input voltage. As the input voltage rises, the current flowing through the common base transistor,  $Q_4$ , decreases.

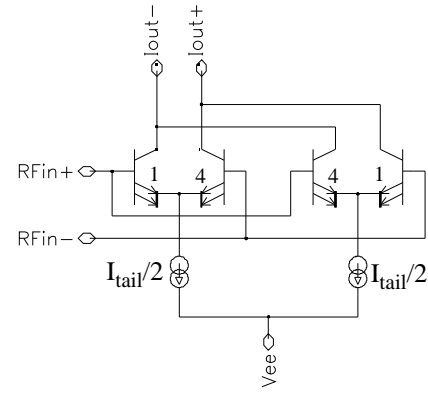


Fig. 2. Cross coupled differential transconductor

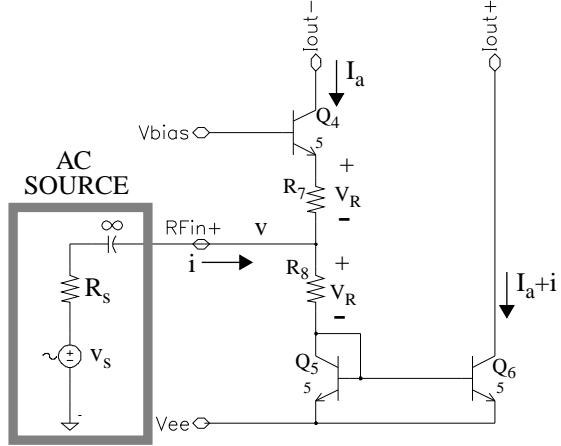


Fig. 3. Linear transconverter

Current flowing through the input of this cell appears as a difference between two output currents,  $I_{Q4C}$  and  $I_{Q6C}$ . The cell thus linearly converts a single ended signal into a differential signal. The purpose of the series resistors,  $R_7$  and  $R_8$ , is to increase the linearity of the cell when driven by a voltage. The mathematical analysis which follows shows that there is a single optimum value for these resistors.

#### IV. ANALYSIS

Define:  $I_q \equiv$  quiescent current in transistors  $Q_4, Q_5$  and  $Q_6$   
 $i \equiv$  delta input current  
 $I_a \equiv$  active current in  $Q_4$   
 $I_a + i \equiv$  active current in  $Q_5, Q_6$   
 $R_s \equiv$  source resistance  
 $R \equiv R_e \equiv$  resistance value of  $R_7$  and  $R_8$   
 $V_s \equiv$  source voltage before source resistance  
 $V \equiv$  delta input voltage  
 $V_R \equiv$  quiescent voltage across  $R_7$  and  $R_8$   
 $V_t \equiv$  thermal voltage =  $kT/q$

Nodal analysis of the circuit depicted in Fig. 3 yields (11).

$$\frac{V}{V_t} = \ln\left(\frac{I_a + i}{I_q}\right) + (I_a + i - I_q)\frac{R}{V_t} \quad (11)$$

This result is based on the assumption that the  $V_{ee}$  bus impedance is negligible and  $V_{bias}$  is driven by an ideal voltage source. A power series expansion of (11) followed by a reversion of series yields (12).

1. Patent Pending, Eric Main and Jeff Durec, February 1994.

$$\frac{i}{2I_q} = \frac{1}{\left(1 + \frac{RI_q}{Vt}\right)} \left( \frac{v}{Vt} \right) + \frac{\left( \frac{1}{2} - \frac{1}{3} \left(1 + \frac{RI_q}{Vt}\right) \right)}{\left(1 + \frac{RI_q}{Vt}\right)^5} \left( \frac{v}{Vt} \right)^3 + \dots \quad (12)$$

This equation can be related to (2) to define the parameters “ $C_n$ ” described in (3). If the input signals (4) in a two tone test are assumed to be equal in amplitude, the input referred third order intermodulation intercept point ( $IP_i^3$ ) can be calculated.  $IP_i^3$  is the input power level at which (13) is satisfied assuming that the third order distortion is the dominant source of the third order intermodulation.

$$IP_i^3 \cong A \left| \left( \frac{3}{4} C_3 A_1^2 A_2 = C_1 A_1 \right) \right|_{A_1 = A_2 = A} = \sqrt[3]{\frac{4 C_1}{C_3}} \quad (13)$$

If  $V_r$  is biased such that (14) is satisfied then third order nulling is achieved (15).  $IP_i^3$  must then be redefined for it will be dominated by fifth order distortion (16). (14) can be satisfied through proper biasing and resistance selection (17).

$$V_r \equiv RI_q = \frac{Vt}{2} \quad (14)$$

$$C_3 = \frac{\frac{1}{2} - \frac{1}{3} \left(1 + \frac{RI_q}{Vt}\right)}{\left(1 + \frac{RI_q}{Vt}\right)^5} \Bigg|_{V_r = \frac{Vt}{2}} = 0 \quad (15)$$

$$IP_i^3 \cong A \left| \left( \frac{5}{4} C_5 A_1^4 A_2 + \frac{15}{8} C_5 A_1^2 A_2^3 = C_1 A_1 \right) \right|_{A_1 = A_2 = A} = \left( \frac{8}{25} \frac{C_1}{C_5} \right)^{1/4} \quad (16)$$

$$R = \frac{Vt}{2I_q} \quad (17)$$

If the RF source applied to the transconverter cell has a finite resistance, third order nulling is maintained with the same value of  $R$  (15).

$$v_s = v + iR_s \quad (18)$$

$$\frac{i}{2I_q} = \frac{1}{\left(1 + \frac{I_q(R + 2R_s)}{Vt}\right)} \left( \frac{v_s}{Vt} \right) + \dots \quad (19)$$

$$\frac{\left( \frac{1}{2} - \frac{1}{3} \left(1 + \frac{RI_q}{Vt}\right) \right)}{\left(1 + \frac{RI_q}{Vt}\right) \left(1 + \frac{I_q(R + 2R_s)}{Vt}\right)^4} \left( \frac{v_s}{Vt} \right)^3 + \dots \quad (20)$$

$$C_3 = \frac{\left( \frac{1}{2} - \frac{1}{3} \left(1 + \frac{RI_q}{Vt}\right) \right)}{\left(1 + \frac{RI_q}{Vt}\right) \left(1 + \frac{I_q(R + 2R_s)}{Vt}\right)^4} \Bigg|_{V_r = \frac{Vt}{2}} = 0 \quad (20)$$

The input resistance of this circuit is calculated in (21). In biasing this circuit, values for  $I$  and  $R_e$  should be chosen such that (22) and (23) are satisfied.

$$R_{in} = (R_7 + re_{Q4}) \parallel (R_8 + re_{Q5}) \quad (21)$$

$$R = R_7 = R_8 = \frac{re}{2} = \frac{2}{3} R_s \quad (22)$$

$$I_q = \frac{Vt}{re} = \frac{3Vt}{4R_s} \quad (23)$$

## V. COMPARISONS

In an attempt to quantify the features of the new transconverter cell, it was compared against the simple differential pair in Fig. 1(A) and the 4 to 1 cross-coupled pair in Fig. 2. In this analysis, the gain cells are driven by a  $50\Omega$  source. Due to their inherently high input impedance the simple differential pair and the cross coupled pair must be terminated in a differential  $50\Omega$  at the input to accommodate a  $50\Omega$  system. The new cell can be set to have  $50\Omega$  input impedance. Each cell was biased at the same total quiescent current. The plots which follow are results of simulations of the MOSAIC V™ high frequency bipolar process.

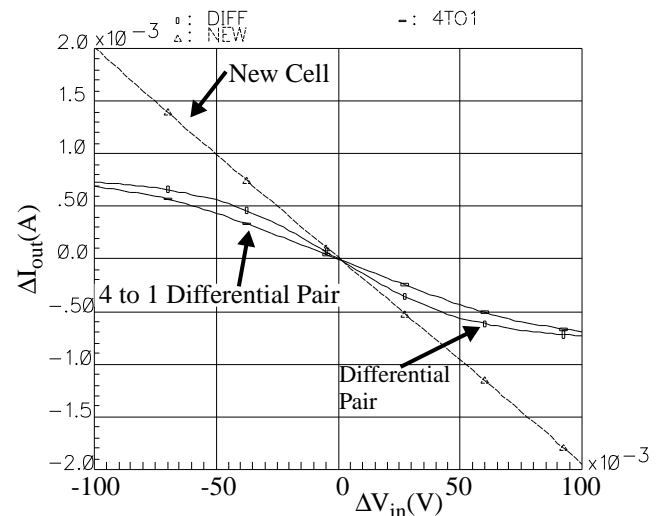


Fig. 4. Delta output current versus delta input voltage (simulated)

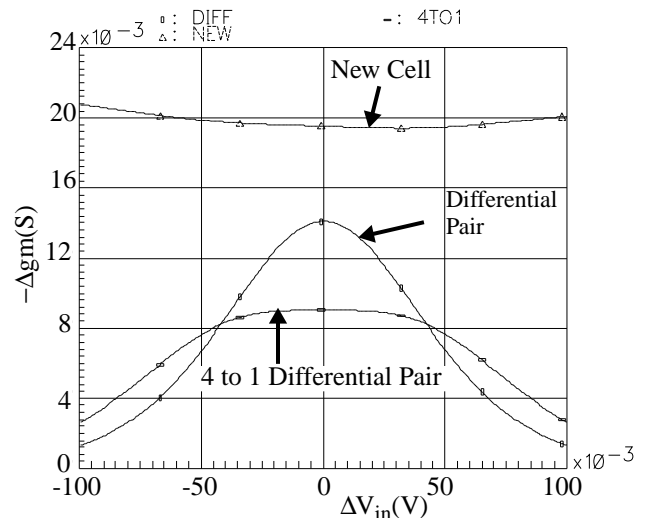


Fig. 5. Incremental transconductance versus delta input voltage (simulated)

Fig. 4 compares the transfer characteristic of the three cells. This graph shows that the new cell is linear beyond  $\pm 100\text{mV}$  input, much greater than the other two gain cells. The improved linearity in the new cell does not come at the expense of transconductance.

The evaluation at zero input of successive derivatives of the transfer function will yield the  $C_n$  coefficients in (3). These coefficients allow for the calculation of the distortion products defined in (7)-(10).

Fig. 5 depicts the first derivative of each transfer characteristic, this is synonymous with incremental gm or transconductance. The transconductance of the new cell is  $\sim 3$ dB greater than that of a simple differential pair. Also, the transconductance of the new cell changes minimally over a large input range. Notice that the cross coupled pair has an improvement in linearity but a reduction in transconductance when compared to a simple differential pair.  $C_1$  for the new cell is shown to be  $\sim 19.5$ mS.

Fig. 6 depicts the second derivative of each transfer characteristic. The flatness of the curve for the new cell implies that it is much less sensitive to input offset.

Fig. 7 depicts the third derivative of each transfer characteristic. Recall, it is the ratio of the third derivative to the first derivative evaluated at zero input which defines  $IP^3_i$

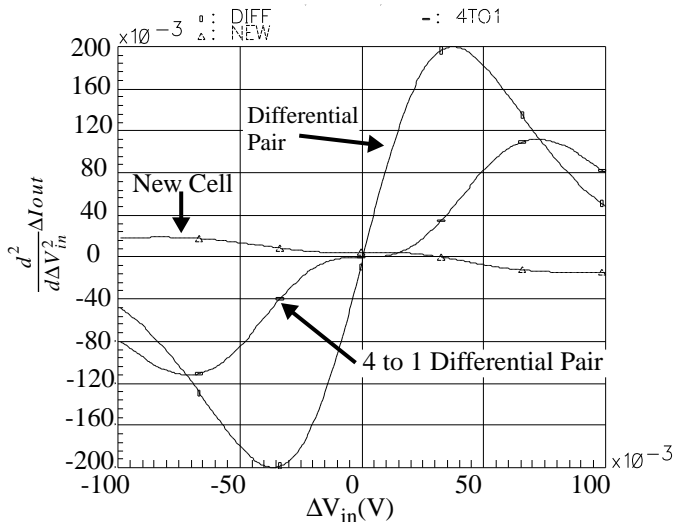


Fig. 6. Second derivative of transfer function versus delta input voltage (simulated)

Both the cross coupled pair and the new cell have third derivatives which, at zero input, evaluate to nearly zero. This translates to infinite  $IP^3_i$  as calculated by (13). Notice that the new cell has a third derivative which is much flatter than the cross coupled pair. This flatness implies that the new cell is very insensitive to input offset.

It has been shown thus far that the new cell has a larger dynamic range of linearity and greater transconductance than both the simple differential pair and the cross coupled pair. What remains to be shown is the impact that each of the three cells have on noise.

Since each cell is being used as a transconductor with an output current for a given input voltage, the output current was converted to a voltage with a noiseless differential  $1\Omega$  transresistance. Fig. 8 shows the noise figure (dB) of each cell plotted versus frequency (Hz). Simulations show the new cell to have a noise figure which is  $\sim 4.4$ dB less than a simple differential pair. The cross coupled pair has a noise figure which is  $\sim 1.6$ dB greater than a simple differential pair. The degradation in noise figure at higher frequencies for the new cell is due to the reduced bandwidth of the cell. The bandwidth in the new cell is limited by the AC performance of the mirror comprised of Q5 and Q6 (Fig. 3).

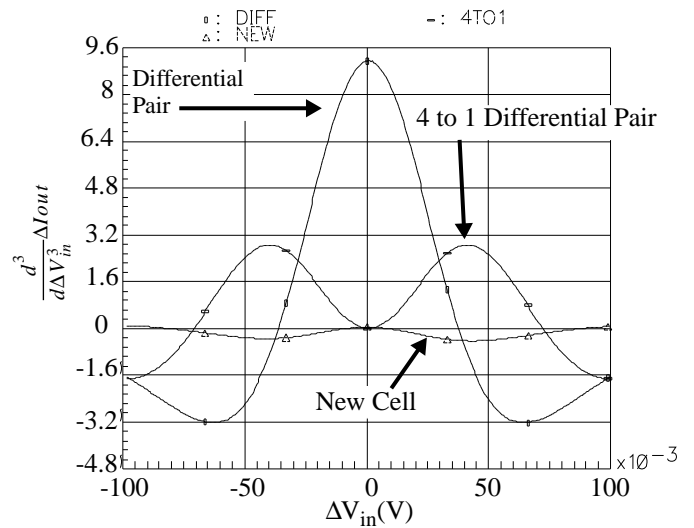


Fig. 7. Third derivative of transfer function versus delta input voltage (simulated)

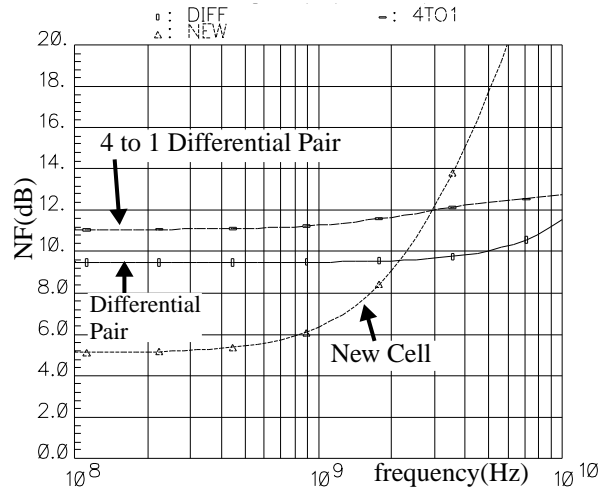


Fig. 8.  $50\Omega$  Noise Figure (dB) versus frequency (Hz) (simulated)

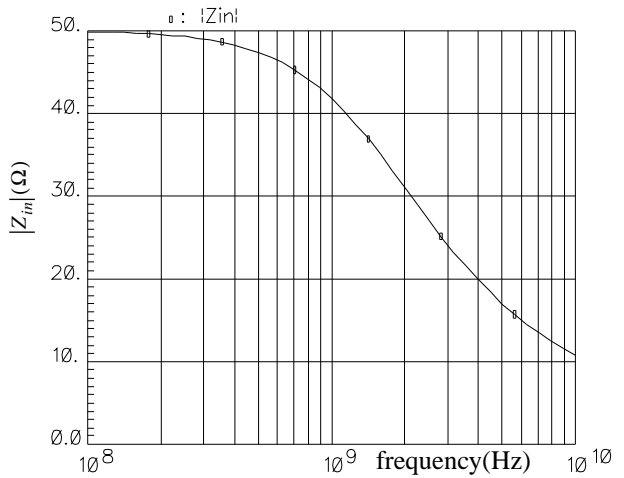


Fig. 9. Magnitude of input impedance versus frequency (Hz) (simulated)

Fig. 9 shows the magnitude of the input impedance plotted versus frequency. This plot proves that the new cell maintains a constant input impedance up to very high frequencies.

The input resistance of the linearized cell changes only slightly as the input voltage varies.. The applied voltage appears at the input of each transconductor and is half the voltage internal to the source<sup>1</sup>. For low distortion operation, the input to output transfer function should be linear over a very wide range of input voltage. The input resistance changes very little even for large input levels. Variations in input resistance with input voltage can cause distortion.

## VI. MEASURED RESULTS

Define:  $I_{in}$   $\equiv$  input current

$V_{in}$   $\equiv$  input voltage

$I_p$   $\equiv$  output current (plus)

$I_m$   $\equiv$  output current (minus)

The linear transconverter was fabricated in the MOSAIC V 0.4 $\mu$ m Bipolar technology. Measured and simulated data are compared in the graphs which follow. A very good correlation between results is evident. The input DC characteristics of the transconverter is shown in Fig. 10. The cell has a linear region greater than  $\pm 400$ mV. The differential output current shown in Fig. 11 maintains the linearity viewed at the input.

The individual differential output currents are plotted in Fig. 12. As the input changes from a negative delta excursion to a positive excursion, one output begins to turn off as the other output current starts to come on. In order to maximize linearity, the transfer of the current from one branch to the other must be optimized. The sum of the output currents is the common mode response as depicted in Fig. 13. This response is the common mode signal which appears at the output.

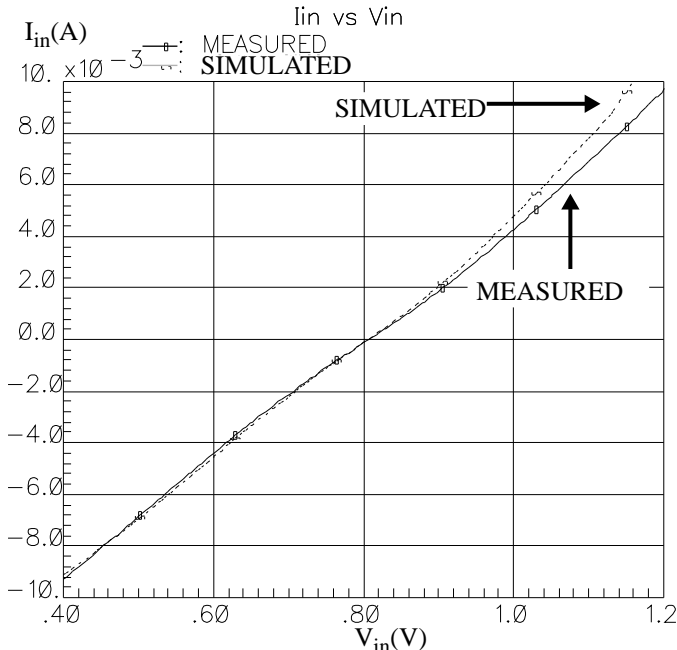


Fig. 10. Input current versus input voltage

1. A voltage source of value  $V_s$  with a source resistance  $R_s$  can be modeled as an ideal voltage source of value  $2V_s$  in series with a resistor of value  $R_s$ . When the source is loaded with a resistance  $R_L$  equal to the source resistance  $R_s$ , a voltage  $V_s$  appears across the load.

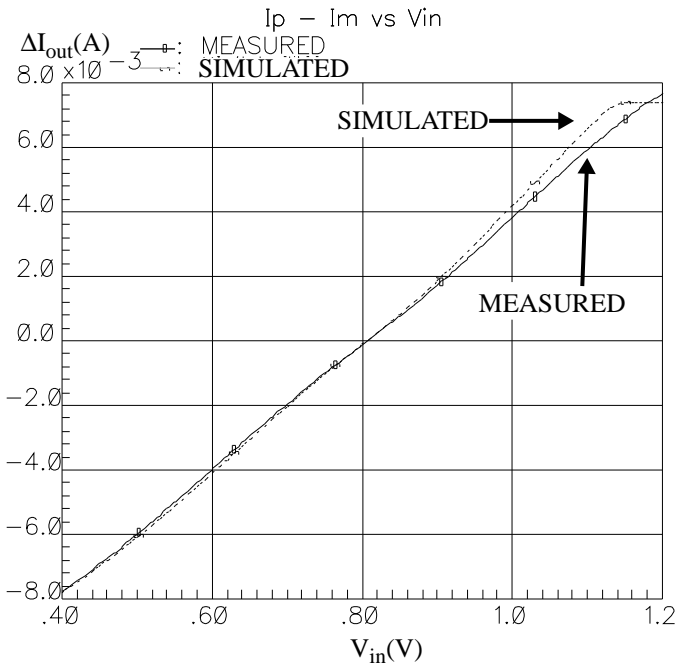


Fig. 11. Differential output current versus input voltage

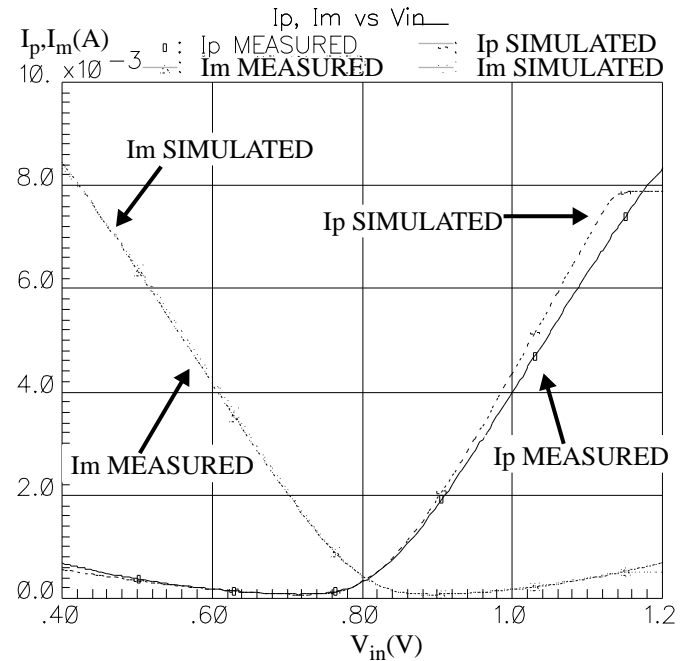


Fig. 12. Plus and minus output currents versus input voltage

Another important facet of the cell is the input impedance and the linearity of the transconductance as the input voltage is varied as shown in Fig. 14. The measured results for both the input resistance and the inverse of the transconductance were measured to be slightly higher (~5%) than the simulated values. This result can easily be explained to be due to Vee bus resistance and/or process variation.

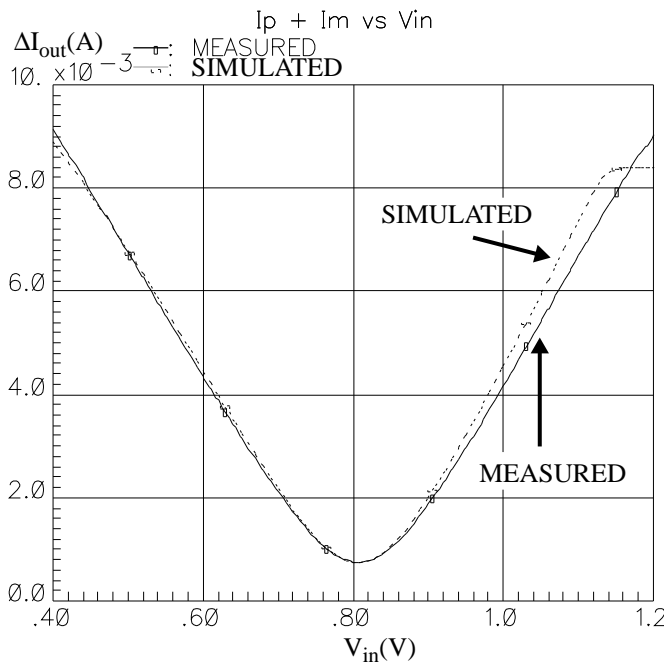


Fig. 13. Common mode output current versus input voltage

The AC performance of the transconductor is shown in Fig. 15. The low frequency roll-off is due to a 100pF AC coupling capacitor. Excellent correlation between the data is maintained even up to 1GHz. The measured 3dB bandwidth of the circuit is 1.8GHz.

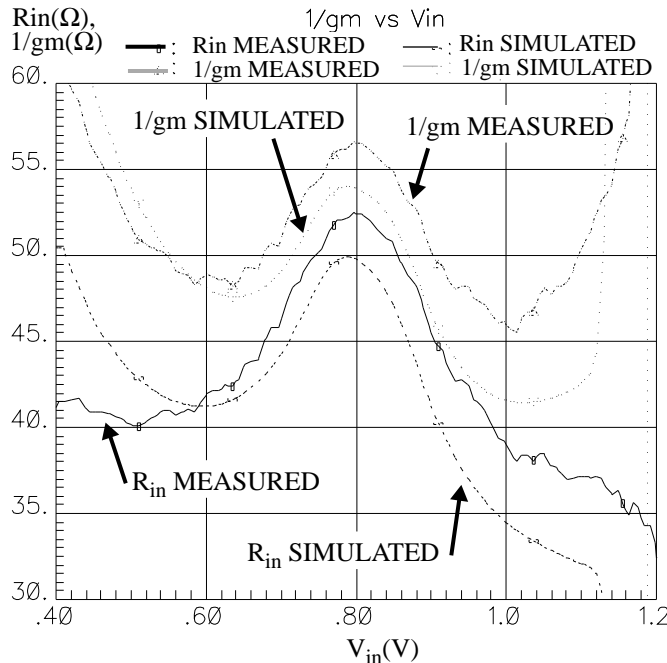


Fig. 14. Input resistance and inverse transconductance versus input voltage

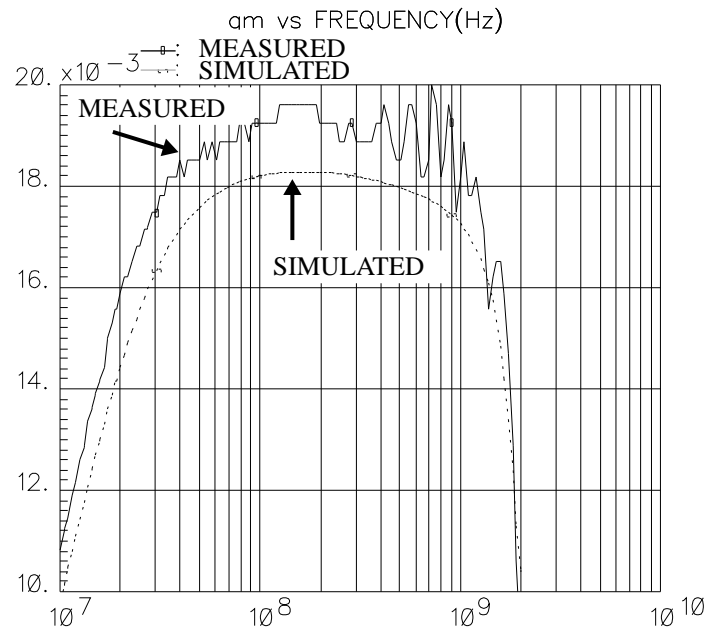


Fig. 15.  $gm(S)$  vs. FREQUENCY(Hz)

## VII. CONCLUSIONS

An improved transconductor cell described has been presented which achieves unprecedented linearity while maintaining a low noise figure and a high transconductance. Linearity is maintained regardless of the source resistance. The measured results of the cell closely match the simulated and theoretical results.

## REFERENCES

- [1] L. W. Couch II, *Digital and Analog Communication Systems*, New York, NY, 1993, pp. 266-272.
- [2] W. E. Sabin, E. O. Schoenike, *Single-Sideband Systems and Circuits*, Macmillan Publishing Company, McGraw-Hill, Inc., New York, NY, 1987.
- [3] R. G. Meyer and W. D. Mack, "A 1-GHz BiCMOS RF Front-End IC," *IEEE J. Solid-State Circuits*, vol. 29, no. 3, pp. 350-355, Mar. 1994.
- [4] H. Sapotta, "Push-Pull Receiver Input Amplifier Stages -- The Solution to Intermod Problems," *Proceedings of the Second Annual WIRELESS Symposium*, pp. 10-11, Feb. 1994.
- [5] H. Sapotta, "Push-Pull AMPLIFIER Stages Quell Receiver Intermodulation Problems," *Wireless Systems Design Technology & Applications*, pp. 5-8, Nov. 1994.